

## Crypt Matching using EACO for Iris Recognition

Z. Zainal Abidin<sup>1</sup>, Z. Abal Abas<sup>2</sup>, R. Ahmad<sup>3</sup>, N. A. Hashim<sup>4</sup> and M. R. Ramli<sup>5</sup>

*Faculty of Information and Communication Technology, Universiti Teknikal Malaysia Melaka,  
Hang Tuah Jaya, 76100, Melaka, Malaysia.*

*Orcid ID: 0000-0003-4868-941X*

### Abstract

Iris recognition has shown a remarkable performance in human identification. To identify a person, IrisCodes is used as a template for comparing a user who is real or vice versa with the stored IrisCodes in a database. **However**, the IrisCodes produces a failure-to-match situation during matching phase and produce non accurate outcome. Consequently, a new method of iris recognition which able to learn human characteristics in natural process and adapt human changes is highly in demand. Studies showed that the nature inspired language has given solutions to overcome the mismatch problem. Ant Colony Optimization (ACO) has been used for iris recognition, but more improvement need to be made. **Therefore**, the purpose of this study is to enhance the ACO technique for better performance. In addition, the iris template consists of unique features such as crypts and furrow, which suitable to be used for matching. The new **method** called as Enhanced Ant Colony Optimization (EACO) creates artificial ants that scan the pixel values according to the range of selected crypt. Then, the scanned pixels value is searched based on degree of angle of ant movements (0°, 45°, 90° and 135°). Besides, the confusion matrix and the blob of iris feature image is indexed before stored the ant feature index (crypt) into the database. For matching, the ant feature index (crypt) is compared at the matching phase to determine the user whether is genuine or not. The **result** shows the Equal Error Rate produces 0.21% that gives lower result from the standard value that is 0.3%. The **impact** of this study produces a cost effective, robustness and lightweight mechanisms as an alternative solution to the current system.

**Keywords:** Crypts; iris recognition; nature inspired language; ant colony optimization.

### INTRODUCTION

Biometric recognition system identify a person's body parts, extract unique features and stored them in a database as a biometric template. Then, when the system is invoked by a user (e.g. a user scans his or her body parts to gain access), the system compares the stored biometric template in the database to provide an indication whether the scanned template matches with the stored template. If matches, then the system allows the user to gain access, else, the system will access denied.

Based on the ISO/IEC2382-37:2012 standard [1], Hamming Distance has been used in the iris recognition's computation with 32-bit for rapid comparisons of IrisCodes through a large database to find a match, which, on a single 300 MHz CPU, such exhaustive searches are performed at a rate of about 100,000 irises per second. In fact, a single 3 GHz server, one million IrisCodes can be compared in about 1 second.

However, when the size of features inside the iris is change due to pupil enlargement for instance, the comparison process produces a failure-to-match problem due to flipping bits situation. The scenario has been difficult to compare unique IrisCodes with the unstable IrisCodes due to changes in iris structure that are affected by the high noise rate in distorted iris, aging, growth, occlusions and health condition. To overcome this problem, the proposed approach did not compare the IrisCodes, but evaluated the iris pixel values. This reason due to this condition is that the pixel values were image based comparison and represented in the unique values of crypts. A considerable amount of literature has been published on swarm intelligence for image based comparison which involves heuristic or random search in order to reduce the FRR and computation time. The goal is to reduce the dimensionality of the feature space, limit storage requirements, removes the redundant, speeding up the computational time of the learning algorithms, improving the data quality, performance enhancement and increasing the accuracy of the resulting approach [2]. Moreover swarm intelligence helps in finding the unique and vital features in natural way. In fact, face [3]–[5], palm print [6] and segmenting authentic iris features [7] have been discovered using ant colony optimization (ACO) [8] and particle swarm optimization (PSO) [9]–[11], for better recognition and classification. In fact, ACO and PSO are useful algorithms due to their capabilities of solving nonlinear and well-constrained problems [12] and useful to find the unique features in the iris structure. However, ACO compares pixel values in iris features in random movements [13] which based on certain patterns [14]. The random movement of ants create longer time for convergence and consume more computational time. On the other hand, ACO is noise tolerance compared to PSO.

Therefore, the image of the iris feature matching approach is introduced in this study. This approach involves ant index feature serves to find similarity in stored iris feature image using Hamming Distance. The testing of matching process was

carried out in CASIA.v3 (high quality image) and UBIRIS.V1 (low quality image) to further evaluate the accuracy (FAR and FRR). The second part evaluates the confusion matrix using long blob matching that provided by the database. Thirdly, the propose approach, EACO is benchmarked with the existing approach, ACO, in terms of accuracy performance which is based on genuien acceptance rate (GAR).

**TEMPLATE MATCHING USING ENHANCED ANT COLONY OPTIMIZATION (EACO)**

The image based matching compares the iris ant feature index (crypt) in the database with newly captured ant feature index (crypt) in matching phase as shown in Figure 1. Two processes involved in iris recognition, which is the enrolment and matching phases.

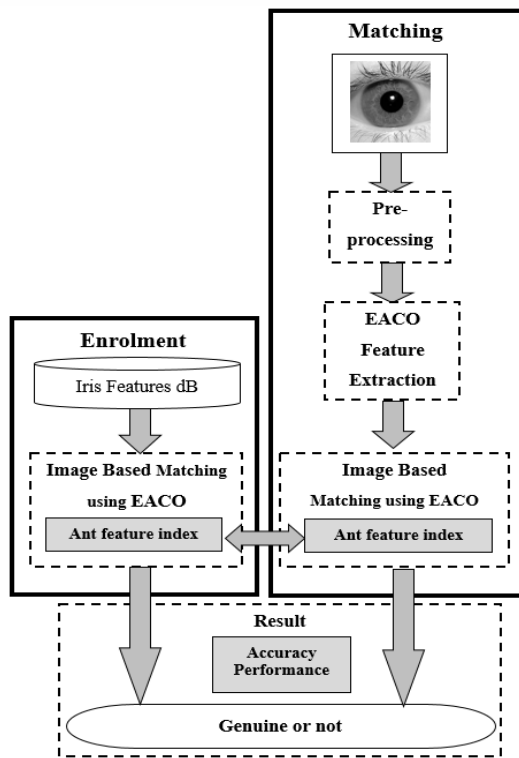


**Figure 1:** Matching with EACO

In the enrolment phase consists of pre-processing (segmentation & normalization), extraction with EACO and store the template into the database in a form of ant feature index (crypt). Meanwhile, the matching process will repeat the enrolment process and compare the ant feature index (crypt) to determine the genuien user.

The *pre-processing* phase uses the Circular Hough Transform (CHT), aims to recognize the circles presented in an iris image. This approach is used to obtain parameters that define the circle which represents the pupil border and the circle that represents the external iris border. The process starts by converting the gray-scaled eye image into a binary edge map. Then, the construction of the edge map is accomplished by the Canny

edge detection with the the incorporation of gradient information. The CHT procedure requires the generation of a vote accumulation matrix with the number of dimensions equal to the number of parameters necessary to define the geometric form. For a circle, the accumulator has 3 dimensions, namely x, y and r. Each edge pixel with coordinates (x, y) in the image space is mapped for the parameters space, determining two of the parameters (for example,  $x_c$  and  $y_c$ ) and finding the third one (for example, r), which resolves the circumference given in Equation 1.

$$(x - x_c)^2 + (y - y_c)^2 = r^2 \tag{1}$$

As a result, the point with coordinates ( $x_c, y_c, r$ ) is obtained in the parameters space, which represents a possible circle in the image. At each set of parameters obtained ( $x_c, y_c, r$ ), the value of the accumulator at the position of A ( $x_c, y_c, r$ ) is incremented. As all pixels have been processed, the highest value of the accumulator indicates the parameters of probable circles in the image. Therefore, the CHT searches the optimum as shown in Equation 2.

$$H(x_c, y_c, r) = \sum_{i=1}^n h(x_i, y_i, x_c, y_c, r) \tag{2}$$

Then, *segmentation and normalization* phases assist the biometric system to locate the almost round shape of an iris, and transform it into the rectangular shape of iris template [20x240] as illustarted in Figure 2.

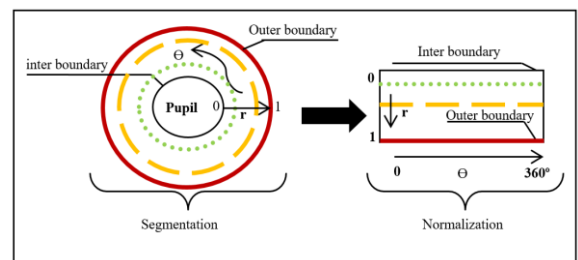


**Figure 2:** Segmentation and Normalization

In addition, iris normalization is the phase based feature extraction method uses one-dimensional (1D) Gabor wavelet for iris template generation which is based on polar coordinates and logarithmic frequency scale. The mathematical form of 1D log polar Gabor filter (Glpr) is described in Equation 3, 4 and 5.

$$Glpr = \exp \frac{(-2\pi^2\sigma^2 (\ln \frac{(r-r_0)}{f})^2 \tau^2)}{(2\ln(f_0 \sin(\theta - \theta_0)))^2} \tag{3}$$

Where,

$$\sigma = \frac{1}{\pi \ln(r_0) \sin \frac{\pi}{\theta_0}} \sqrt{\frac{\ln 2}{2}} \tag{4}$$

$$\tau = \frac{2\pi \ln(r_0) \sin(\pi / \theta_0)}{\ln 2} \sqrt{\frac{\ln 2}{2}} \tag{5}$$

Where,

( $r, \sigma$ ) = polar coordinates

$(r_0, \theta_0)$  = initial values,

$f$  = center frequency of the filter

$f_0$  is the parameter that controls the bandwidth of the filter.

In the *extraction* phase, extraction approach firstly starts with the iris template [20x240] that is divided into three main regions since there is natural of biological regions exist in the ciliary zone. The region '1' comprises mostly furrow, region '2' contains many crypt and region '3' holds eyelids and eyelashes. Only region '1' and '2' are selected for recognition since eyelashes and eyelids are not in this scope of study.

Moreover, the iris feature has special regions according to the type of blob features for instance, crypt, radial furrow and pigment melanin in the ciliary zone. Based on the natural region, average length of rows for crypt is transformed into mathematical operations to find the approximation of rows for crypt using mean formula as shown in Equation 6. The purpose of measuring the length of rows inside the iris feature template is to determine the filter size for crypt.

$$\bar{x} = \frac{\sum X}{n} \quad (6)$$

Where,

$\bar{x}$  = mean

$\sum X$  = Sum of occurrences

$n$  = Total number of occurrences

Nevertheless, the filter size is based on assumption made in conditions of an eye is in a normal condition, where eyes were taken from the quality iris dataset, that is from CASIA.v3.

Secondly, ant searches the unique features in the iris texture [20x240] using angle of degree (0°, 45°, 90°, 135° and 180°) and begin from left most point in the feature space as shown in Figure 3.

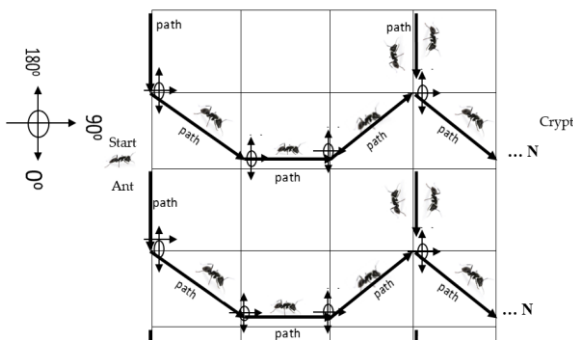


**Figure 3:** Ant Movement based on Degree of Angle

Thirdly, the movement of ants followed in the zig zag manner till to the end of the space and it continues for the specified number of iterations until to the end of the matrix in order to

obtain a convergence. The equation for performing iteration for finding crypt is as in Equation 7.

For  $k = 0$ ,

$$\theta_{path\_crypt} \begin{cases} 0^\circ & \text{if } i = 1, 3 \ \& \ j = 1 + 3k \\ 45^\circ & \text{if } i = 2, 4 \ \& \ j = 1 + 3k \\ 90^\circ & \text{if } i = 2, 4 \ \& \ j = 2 + 3k \\ 135^\circ & \text{if } i = 2, 4 \ \& \ j = 3 + 3k \\ 180^\circ & \text{if } i = 1, 3 \ \& \ j = 3 + 3k \end{cases} \quad (7)$$

Where iteration =  $k + 1$ .

Once the unique features are found, the ant finds the crypt at the interest regions number 2 as shown in Figure 4.

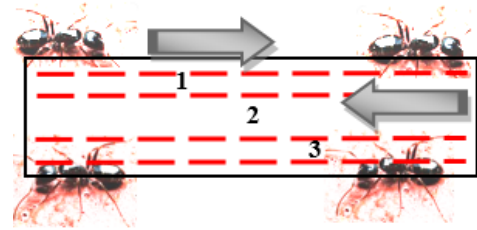


**Figure 4:** Ant Movement in the Interest Region

Fourthly, the artificial ant to decide from one point to another point, if an ant is in point  $i$ , it chooses the next point  $j$ . Based on position of  $j$ , artificial ant moves according to a angle of degree as stated in Equation 8 and 9, where  $d \in [1, N]$  ( $N$  is the total points in the iris search region) that, each pair of wise point ( $i, j$ ) has  $(N-1) + (N-2) + \dots + 2 + 1$  trail values with one for each possible destination point  $d$ , an ant located in point  $i$ , can have self-determining to the final destination. Therefore, the ants adapt their self-searching activity to the varying point characteristics ( $P_d$ ) is in Equation 8.

$$P_d = \sum_{d'=1}^N \frac{f_j d'}{2} \quad (8)$$

The angle in degrees (0°, 45°, 90° and 135°),  $P_d$  is a binary label, valued in {0, 1} and the degree vector  $X = (X(1), \dots, X(q))$  models some multivariate observation for predicting  $P_d$ , taking its values in a high-dimensional space as described in Equation 9.

$$X \subset R_q, q \geq 1. \quad (9)$$

The probability measure on the underlying space is entirely described by the pair  $(m, n)$ , where  $m$  denotes the marginal distribution of  $X$  and  $n(x)$  is the posterior probability as shown in Equation 3.10.

$$n(x) = \sum_{m \in N_k} \{P_{nd} = 1, | X = x\} \quad (10)$$

In maintaining the pheromone trail,  $\tau_k$ , the ant relies on a fortification planning. In the context of this study, fortification planning was a back-up plan if the current pheromone update modification did not succeed. The returning mediator update the pheromone for destination  $d'$ , the probability  $P_{fd}'$ , according to Equation (4). The factor  $r$  is an edge of region value;  $r \in (0,1)$  used by the current point for positive

fortification is in Equation 11.

$$Pfd' \leftarrow Pfd' + r(1 - Pfd') \quad (11)$$

The negative fortification is important for erasing the pheromone in local iris map, which is the unnecessary trail made that has been deleted. In this study, if there is a pair wise of points blurred or damaged, it helps in learning a new pairwise points from one point to the destination point, or else the pheromone update trail is ended in the system. When all ants have completed a solution, the trails are updated by the Equation 12.

$$\tau_{xy} \leftarrow (1 - \rho) \tau_{xy} + \sum_k \Delta \tau_{xy}^k \quad (12)$$

where

$\tau_{xy}$  = the amount of pheromone for state transition  $xy$ ,

$\rho$  = the pheromone evaporation coefficient

$\Delta \tau_{xy}^k$  = the amount of pheromone by  $k$ th ant, given for moves corresponding to the edge of region map by using Equation 13.

$$\Delta \tau_{xy}^k = \begin{cases} I \equiv Q/Lk & \text{if ant } k \text{ uses curve } xy \text{ in its tour} \\ 0 & \text{otherwise} \end{cases} \quad (13)$$

Where

$Lk$  = cost of the  $k$ th ant's tour (typically the distance of end to end points)

$Q$  = constant.

$\Delta \tau_{xy}^k$  determines the values in the interest region

$Qk$  is equal to  $I$  from Equation 12. If ant  $k$  matches with  $k-1$  iris feature at  $xy$ , the enhanced ant colony optimization pheromone table is updated, else vice versa. The ants' movements are based on the precision (FAR and FRR) in order to obtain GAR. Then, the confusion matrix shows the evaluation function of the feature subsets which are crypt and non crypt features. The value of the ant feature index (crypt) is stored into the database for the next matching process and the illustrated as in Figure 5.



Figure 5: Ant Feature Index Crypt

Meanwhile, another process in iris recognition is the matching phase, which, the iris features images are indexed by ant feature vector (stored as an index in feature databases) as crypt index. The similarity of the feature index vectors of the query and database images is measured to retrieve the image. Let  $\{F(x, y); x = 1, 2, \dots, X, y = 1, 2, \dots, Y\}$  be a two-dimensional image pixel array. For black and white images,  $F(x, y)$  denotes the grayscale intensity value of pixel  $(x, y)$ . The problem of retrieval is following: For a query image  $Q$ , we find image  $T$  from the image database, such that distance between corresponding feature vectors is less than specified threshold, i.e.,  $D(\text{Feature}(Q), \text{Feature}(T)) \leq t$  (1). The co-occurrence matrix  $C(i, j)$  counts the co-occurrence of pixels with gray values  $i$  and  $j$  at a given distance  $d$ . The distance  $d$  is defined in polar coordinates  $(d, \theta)$ , with discrete length and orientation. In practice,  $\theta$  takes the values  $0^\circ; 45^\circ; 90^\circ; 135^\circ$  and  $180^\circ$ .  $G$  is the number of gray-values in the image, then the dimension of the co-occurrence matrix  $C(i, j)$  is  $N \times N$ .

## EXPERIMENT ENVIRONMENT

The experiments were carried out over the course of two different iris databases which is CASIA.v3 (high quality images) and UBIRIS.v1 (low quality images). This experiment was repeated under conditions in which the iris database is divided into two sets of iris feature images. The first set contains training set of 60% iris images while testing set contains 40% images. The following Table 1 explains the iris database classification for image based comparison.

Table 1: Iris Database Classification

Iris Database	Total Iris Image	Training	Testing
CASIA.V3 (High quality)	10	6	4
UBIRIS.V1 (Low quality)	5	3	2

The training set is used to represent the genuine models of iris images. For validation, the testing set of iris feature images are used to obtain the accuracy performance. The number of the selected features and the quality of the classification results are considered for performance evaluation.

The experiment was conducted using similar testbed and tools with ACO. Moreover, samples of data testing for matching has been provided for verification process. In finding the optimal solution, the configuration of parameter settings across a range of values must be determined. The number of particles (population) was set to 5, 20 and 100. The various sizes of particles are for the comparison purposes. The maximum generation (iteration) and fitness function were set to 100 and 0.95 respectively. Meanwhile, the cognitive learning factor ( $C1$ ) and the social learning factor ( $C2$ ) were between 0.1 and 0.2 since the addition of both values, ( $C1+C2$ ) giving a limited

value of 4. Therefore, the following parameters for the experimental setup are:

- $\alpha$  = number of ant for movements (for training)
- $\beta$  = number of ant for movements (for testing)
- $\rho$  = pheromone settings value
- $\pi$  = radius of ant's coverage from one space to another space
- ant memory buffer = temporary memory location to store latest information
- clique mode = the arc of the complete convergence
- pheromone intensity of each arc is equal to 1
- m = the number of ant in each iteration
- i = number of iteration
- k = the maximum iterations

The experiments are designed to be conducted based on parameters leading to a better convergence which are tested and the best parameters that are obtained by simulations are as follows:  $\alpha=1$ ,  $\beta=2$ , evaporation rate  $\rho=0.95$ , the initial pheromone intensity of each arc (seed) is equal to 1, the number of ant in each iteration  $m = 2, 4, 6, 8$  and  $10$ , and the maximum iterations  $k=50$ .

To evaluate the average classification accuracy of the selected feature subsets, 10-fold cross validation (CV) is used. The EACO has one arc; it means that ant moves forward and backward in the same route. The iteration of ant's movements in the same path is done until the searching process is converged. The parameter of precision is used to measure the convergence in the searching space. The best precision values determine the most accurate point. Accuracy is assumed to be high since the artificial ant makes a decision which path to follow if simultaneous searching point occurred. The accuracy rates determine whether the proposed approach correctly selects the crypt features. Thus, Hamming distance (HD) is the matching operator in evaluating the ant features index (crypt) in iris template since it evaluates the number of scores. After the iris feature is indexed, the feature index images are stored in the database.

**EXPERIMENT RESULTS**

Several experiments have been conducted in this study, Firstly, experiment to prove the failure-to-match situation by comparing the existing method (Libor Masek[15]) that using IrisCodes and EACO which using iris features. The procedures and explanation of failure-to-match has been mentioned as approaches are executed using the same iris database that is CASIA.v3 and UBIRIS.v1 to avoid biasness. Secondly, the experiment is implemented in finding the accuracy

performance between ACO and EACO through the percentage of GAR differences before and after the matching process.

Figures 6 and 7 show two iris images from two different individual, which indicates that there is “3 person in DB” means, user number three (No.3) out of all 240 users in the database. Thus, Figures 6 indicates that the system detected User A as person number three (No. 3) in the database.

*A. Experiment 1*

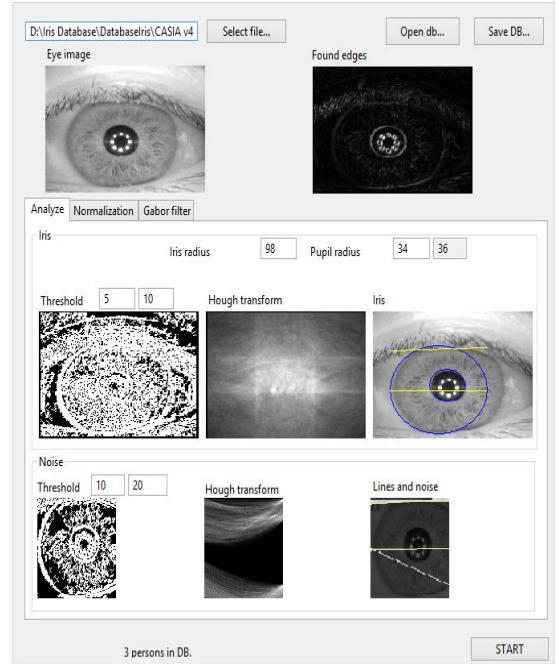


**Figure 6:** IrisCodes using Libor Masek for User A.

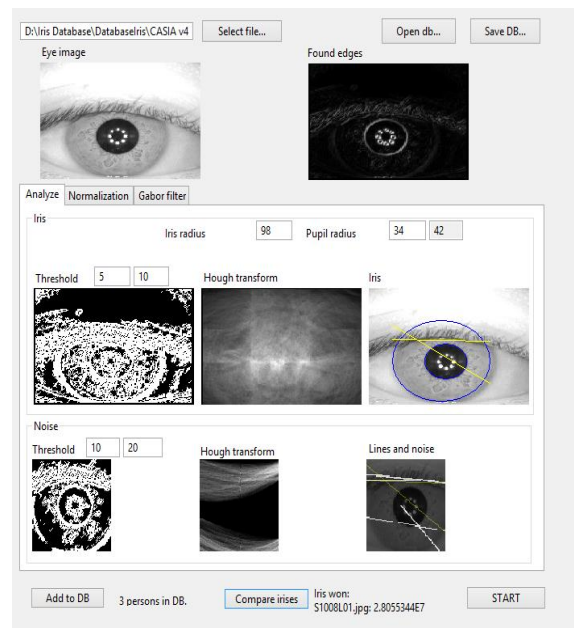


**Figure 7:** IrisCodes using Libor Masek for User B.

Suprisingly, Figure 7 shows that the system detected User B as the same as the person detected in Figure 6, which indicates that different iris images but referring to the same user, who is (No.3). Therefore, this result showed that Libor Masek’s iris recognition approach has a failure-to-match issue.

Oppositely, the experiment is conducted using the same iris images and performed using EACO as in Figures 8 and 9. The outcome of experiments indicate that two different person has been detected and there was no miss match problem in the new approach.

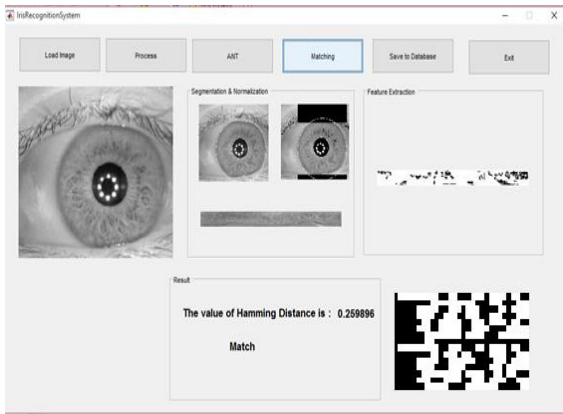


Figure 8: EACO with User A

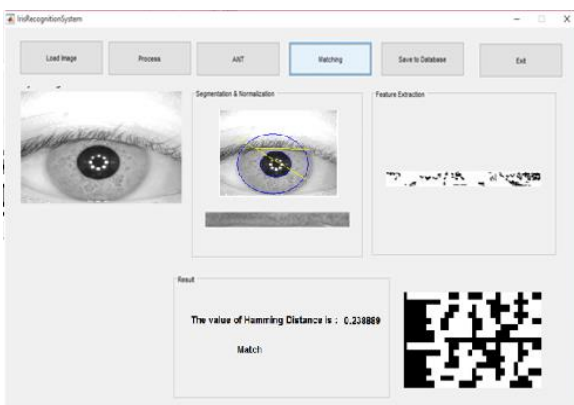


Figure 9: EACO with User B

The best crypt and radial furrow shapes located in the iris feature are extracted and stored the important information into the feature index format called as ‘Ant Feature Index’

According to biometrics standard, that is ISO/IEC 2382-37:2012, the value of FAR is fixed at 0.1% using Hamming Distance as an indicator for verification performance. To determine a genuine, the Hamming Distance (HD) is between 0 to 0.3 and “Match” result is appeared on the screen to indicate that the matching process is successful. Meanwhile, if Hamming Distance shows the result is more than 0.3, it determines the user is not a genuine and the result is “Non Match”.

Figure 10 indicates that Hamming Distance is 0.238889 and produces a ‘Match’ result which stated that the user is genuine.

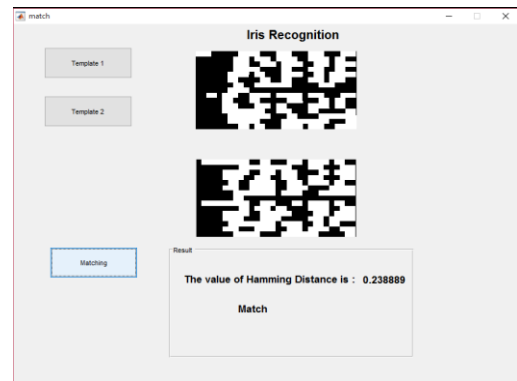


Figure 10: Ant Feature Indexed based on Hamming Distance

### B. Experiment 2

Based on the bar graph, the experiment results show that GAR values contribute less differences compared to after matching process when EACO was searching for crypt in CASIA.v3 and UBIRIS.v1. The experiment results were 81.95% decreased from 82.86% and 56.25% to 53.07%. The outcome of this experiments indicates that the small change of GAR value proven the robustness of EACO in detecting the genuien user eventhough before and after the matching process. The before matching means the training process that has been done after the EACO extraction phase and after matching refers to testing process to determine the GAR(%) values at earlier stages of this study. Furthermore, in UBIRIS.v1 database, EACO ables to recognize iris images (crypt) in lower quality images since only 3.18% varies in searching the crypts.

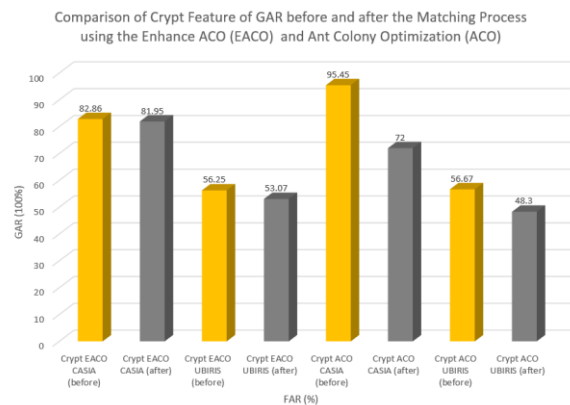


Figure 11: GAR before and after matching

Suprisingly, ACO performs a huge different before and after the matching process. The GAR value is 95.45% is obtained during the training however the GAR gives 72% at the testing stage, that indicates a low accuracy rate. Nevertheless, ACO able to search for iris features under low quality image since before the matching the GAR is 56.67% but after the matching process the GAR produces 48.3%.

## CONCLUSION

In this study, an improved image based matching approach is proposed for iris recognition. The EACO is designed to extract the unique iris features such as crypt and furrow for better detection. Iris features is partitioned into region of interest based on biological structure of the iris features itself. The iris texture with [20x240] is divided into 3 regions of interest in order for ants to self-learning in finding the unique iris features (crypt). The region '1' contains the radial furrow, the '2' consists of crypt and '3' contains the eyelashes and eyelids. Only region '1' and '2' is selected for iris feature extraction. Then the ant searches the unique features in the iris template [20x240] using angle of degree (0°, 45°, 90°, 135° and 180°) and starts from left upper most point until to the end of the matrix in zig-zag manner. After that, ants' movements are measured with the precision (FAR and FRR) which based on EACO Pheromone Table. Both ants stop at 10<sup>th</sup> iterations or once converged. The confusion matrix shows the evaluation function of the feature subsets which are crypt and non crypt features. Lastly, crypt features is indexed in order to store into the database for future matching process. In order to evaluate the EACO with ACO, the matching process has been done in (high quality images), that is CASIA.v3 and (low quality images), which is UBIRIS.v1 databases. The result shows the Equal Error Rate produces 0.21%, lower result from the standard value that is 0.3%. However, the accuracy performance of EACO produces on average of 76% to 84% which still indicates low accuracy performance. On the other hand, the impact of this study produces a cost effective, robustness and lightweight mechanisms.

## ACKNOWLEDGEMENT

A special thanks to Ministry of Higher Education or Kementerian Pendidikan Tinggi (KPT), Universiti Teknikal Malaysia Melaka (UTeM) and Centre for Research and Innovation Management (CRIM) sponsor this research through the Fundamental Research Grant Scheme (FRGS) (Grant No. FRGS/1/2015/ICT04/FTMK/03/F00287). Thank you to friends and staff from Faculty of Information and Communication Technology (FTMK) for giving support to complete this project. A highly appreciation to CASIA and UBIRIS for sharing iris images.

## REFERENCES

- [1] ISO/IEC, *Biometrics*, vol. 2382–37. Switzerland, 2012, p. 28.
- [2] L Ladha and T. Deepa, "Feature Selection Methods and Algorithms," *Int. J. Comput. Sci. Eng.*, vol. 3, no. 5, pp. 1787–1797, 2011.
- [3] S. Venkatesan and S. S. R. Madane, "Face Recognition

System with Genetic Algorithm and ANT Colony Optimization," *Int. J. Innov. Manag. Technol.*, vol. 1, no. 5, pp. 469–471, 2010.

- [4] M. M. Kabir, M. Shahjahan, and K. Murase, "A new hybrid ant colony optimization algorithm for feature selection," *Expert Syst. Appl.*, vol. 39, no. 3, pp. 3747–3763, Feb. 2012.
- [5] E. Grosso, L. Pulina, and M. Tistarelli, "Modeling biometric template update with Ant Colony Optimization," *2012 5th IAPR Int. Conf. Biometrics*, pp. 506–511, Mar. 2012.
- [6] D. R. Kisku, P. Gupta, J. K. Sing, and C. J. Hwang, "Multispectral Palm Image Fusion for Person Authentication Using Ant Colony Optimization," in *2010 International Workshop on Emerging*
- [7] N. K. Ratha, J. H. Connell, and R. M. Bolle, "Enhancing security and privacy in biometrics-based authentication systems," *IBM Syst. J.*, vol. 40, no. 3, pp. 614–634, 2001.
- [8] L. Ma, K. Wang, and D. Zhang, "A universal texture segmentation and representation scheme based on ant colony optimization for iris image processing," *Comput. Math. with Appl.*, vol. 57, no. 11–12, pp. 1862–1868, Jun. 2009.
- [9] V. P. Sharma, S. K. Mishra, and D. Dubey, "Improved Iris Recognition System Using Wavelet Transform and Ant Colony Optimization," in *IEEE 2013 5th International Conference on Computational Intelligence and Communication Networks*, 2013, pp. 243–246.
- [10] B. Logannathan, "Iris authentication using pso," *Int. J. Comput. Organ. Trends*, vol. 2, no. 1, pp. 10–15, 2012.
- [11] H. Ghodrati, S. Member, M. J. Dehghani, and H. Danyali, "Iris Feature Extraction Using Optimized Gabor Wavelet Based on Multi Objective Genetic Algorithm," in *IEEE*, 2011, pp. 159–163.
- [12] Y. Chen, Y. Liu, X. Zhu, F. He, H. Wang, and N. Deng, "Efficient iris recognition based on optimal subfeature selection and weighted subregion fusion.," *ScientificWorldJournal.*, vol. 2014, no. 2, p. 157173, Jan. 2014.
- [13] D. Rai and K. Tyagi, "Bio-inspired optimization techniques," *ACM SIGSOFT Softw. Eng. Notes*, vol. 38, no. 4, pp. 1–7, Jul. 2013.
- [14] D. M. Rankin, B. W. Scotney, P. J. Morrow, and B. K. Pierscionek, "Iris recognition—the need to recognise the iris as a dynamic biological system: Response to Daugman and Downing," *Pattern Recognit.*, vol. 46, no. 2, pp. 611–612, Feb. 2013.
- [15] L. Masek, "Recognition of Human Iris Patterns for Biometric Identification," *The University of Western Australia*, 2003.